ADVANCED MATERIALS

Experimental

GCNBs were prepared by chemical vapor deposition at Tokai Carbon Co. Ltd. The detailed preparation procedure has been reported previously [18]. The structure of GCNBs was studied by X-ray diffraction (XRD) (Rigaku, Rint2500), Raman spectroscopy (Jovin-Yvon, T-64 000), and TEM (Hitachi-9000).

For the fabrication of GCNB electrodes, each GCNB sample was mixed with a solution of poly(vinylidene difluoride)/*N*-methylpyrrolidinone (PVdF/NMP) (KF # 1120, Kureha) to make a slurry of a suitable viscosity. The weight ratio of GCNBs to PVdF was adjusted to 9:1. Then, the slurry was spread onto a copper foil thinly and evenly to fabricate the electrodes. The electrode was allowed to stand in a draft overnight to evaporate most of the NMP solvent, and was then vacuum dried at 80 °C for 1 day. The electrode thickness was ca. 100 μm. For electrochemical measurements, 1 mol dm^{-3} $LiClO_4$ dissolved in PC and 1 mol dm^{-3} $LiClO_4$ dissolved in EC:DEC (1:1 by volume) were used as electrolytes. The former and the latter electrolytes are referred to as PC- and EC-based electrolytes, respectively. CV measurements were performed in a three-electrode cell using a HSV-100 (Hokuto Denko) instrument. Alternating current (AC) impedance measurements were also conducted with a three-electrode cell using a Solartron SI 1255 impedance analyzer coupled with a SI 1480 multi-channel electrochemical interface over a frequency range from 100 kHz to 10 mHz with an AC oscillation of 10 mV. Lithium metal was used as the counter and reference electrodes, and the GCNB electrode served as the working electrode. Unless otherwise stated, potentials were referenced to lithium metal.

Received: February 14, 2005
Final version: July 13, 2005
Published online: October 27, 2005

[1] T. Abe, H. Fukuda, Y. Iriyama, Z. Ogumi, *J. Electrochem. Soc.* **2004**, *151*, A1120.
[2] Y. Iriyama, H. Kurita, I. Yamada, T. Abe, Z. Ogumi, *J. Power Sources* **2004**, *137*, 111.
[3] I. Yamada, T. Abe, Y. Iriyama, Z. Ogumi, *Electrochem. Commun.* **2003**, *5*, 502.
[4] T. Doi, K. Miyatake, Y. Iriyama, T. Abe, Z. Ogumi, *Carbon* **2004**, *42*, 3183.
[5] T. Doi, Y. Iriyama, T. Abe, Z. Ogumi, *Anal. Chem.* **2005**, *77*, 1696.
[6] M. Morita, N. Nishimura, Y. Matsuda, *Electrochim. Acta* **1993**, *38*, 1721.
[7] N. Takami, A. Satoh, M. Hara, T. Ohsaki, *J. Electrochem. Soc.* **1995**, *142*, 371.
[8] M. D. Levi, D. Aurbach, *J. Phys. Chem. B* **1997**, *101*, 4641.
[9] A. Funabiki, M. Inaba, Z. Ogumi, S. Yuasa, J. Otsuji, A. Tasaka, *J. Electrochem. Soc.* **1998**, *145*, 172.
[10] J. Barker, R. Pynenburg, R. Koksbang, M. Y. Said, *Electrochim. Acta* **1996**, *41*, 2481.
[11] H. Sato, D. Takahashi, T. Nishina, I. Uchida, *J. Power Sources* **1997**, *68*, 540.
[12] D. Aurbach, M. D. Levi, E. Levi, H. Teller, B. Markovsky, G. Solitra, U. Heider, L. Heider, *J. Electrochem. Soc.* **1998**, *145*, 3024.
[13] Y. Iriyama, M. Inaba, T. Abe, Z. Ogumi, *J. Power Sources* **2001**, *94*, 175.
[14] A. N. Dey, B. P. Sullivan, *J. Electrochem. Soc.* **1970**, *117*, 222.
[15] C. Ho, I. D. Raistrick, R. A. Huggins, *J. Electrochem. Soc.* **1980**, *127*, 343.
[16] G. C. Chung, *J. Power Sources* **2002**, *104*, 7.
[17] M. Inaba, Z. Siroma, A. Funabiki, Z. Ogumi, T. Abe, Y. Mizutani, M. Asano, *Langmuir* **1996**, *12*, 1535.
[18] Y. Yamamoto, T. Tahara, R. Harada, *Japanese Patent 2003-1803*, **2003**.

Nanomechanical Architecture of Strained Bilayer Thin Films: From Design Principles to Experimental Fabrication**

By *Minghuang Huang*, *Carl Boone*, *Michelle Roberts*, *Don E. Savage*, *Max G. Lagally*, *Nakul Shaji*, *Hua Qin*, *Robert Blick*, *John A. Nairn*, and *Feng Liu**

Nanofabrication and nanosynthesis have become some of the most active research areas in recent years. Certain classes of nanostructures have been successfully fabricated in bulk or grown on surfaces by self-assembly and self-organization processes,[1–3] sometimes combined with lithographic patterning.[4] However, very often the nanostructures are made in an empirical manner lacking a sufficient level of control. Despite the enormous success we have enjoyed so far, such as with carbon nanotubes[1,5] and zinc oxide nanobelts,[2] nanofabrication and synthesis with most materials are still very difficult. There exists a strong need for the development of nanofabrication techniques with a higher degree of control over size and geometry as well as with a high degree of versatility applicable to different materials. Here, we demonstrate the generic design principles of an emerging nanofabrication approach based on *nanomechanical architecture* of strained bilayer thin films. It allows fabrication of a variety of nanostructures, such as nanotubes, nanorings, nanodrills, and nanocoils, using combinations of different materials with an unprecedented level of control.

Like a bimetallic strip in a thermostat that bends due to different thermal stress in the two metal layers, a strained bilayer thin film bends due to lattice-misfit strain in the two layers. In particular, when the film thickness is reduced to the nanometer scale, its bending magnitude can be so large so that it can fold into tubular shapes with multiple turns as the film length becomes longer than $2\pi R_0$, where R_0 is the characteristic radius of curvature of the bending film. Remarkably, this simple bending phenomenon has recently been exploited for fabricating a variety of nanostructures, including nanotubes,[6–10] nanorings,[11–13] nanodrills, nanocoils,[6,14] nano-

[*] Prof. F. Liu, M. Huang, C. Boone, Prof. J. A. Nairn
Department of Materials Science and Engineering
University of Utah, Salt Lake City, UT 84112 (USA)
E-mail: fliu@eng.utah.edu
M. Roberts, Dr. D. E. Savage, Prof. M. G. Lagally
Department of Materials Science and Engineering
University of Wisconsin, Madison, WI 53706 (USA)
N. Shaji, Dr. H. Qin, Prof. R. Blick
Department of Electrical and Computer Engineering
University of Wisconsin, Madison, WI 53706 (USA)

[**] F. Liu thanks O. Schmidt for helpful comments on the manuscript. The authors acknowledge the continuous support from DOE and NSF.

  DOI: 10.1002/adma.200501353

rods,[12] and nanomirrors.[15,16] Figure 1 shows examples of an array of nanorings (Fig. 1a), a nanodrill (Fig. 1b), and a nanocoil (Fig. 1c), all formed from strained Si/SiGe bilayer films.[17]

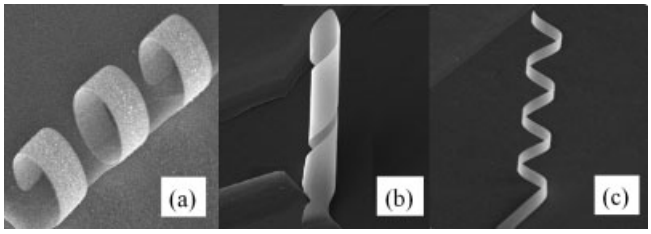

Figure 1. Scanning electron microscopy images of nanoarchitectures fabricated from strained Si/SiGe bilayer films: a) Nanorings with a thickness of 80 nm, radius of ~3.0 μm, and width of 3 μm; b) nanodrill with a thickness of 110 nm, radius of ~2.4 μm, and width of 10 μm; and c) nanocoil with a thickness of 110 nm, radius of ~2.4 μm, and width of 2 μm. In general, we can vary the thickness from 10 to 200 nm and length and width from 20 nm to 100 μm.

All these different classes of nanostructures are formed by the same mechanism—namely, the tendency of strained bilayer films to bend (or to fold). We therefore name these the "nanomechanical architectures" of strained bilayer thin films. One outstanding advantage of this nanofabrication technique is its versatility. Not only can a variety of nanomechanical architectural designs be made, but they can also be made with different materials, including semiconductors, metals, and insulators, as well as combinations of these materials. Furthermore, in principle, a high degree of control should be achievable. Not only can different nanoarchitectures be designed, but also their size and shape can be tuned over a wide range by choosing different combinations of materials, varying film dimensions, and applying external forces. This approach also makes it possible for parallel mass production of identical or different nanostructures.

The promising potential shown by this novel and fascinating approach has attracted a lot of recent interest.[6–16] However, the work to date remains largely empirical; most structures are made by trial and error. This is mainly due to the lack of complete understanding of the underlying physical principles, which hinders a higher degree of experimental control. Here, we theoretically analyze and experimentally demonstrate fundamental mechanisms governing the nanomechanical architecture of strained bilayer nanometer-thick thin films. We establish certain generic design principles, which will lead to selective fabrication of different classes of nanostructures, such as nanotubes and nanorings versus nanodrills and nanocoils, in a controllable manner. Our analysis will be based on a continuum-mechanics theory for systems where the atomic structures and surface/interface effects are not yet important.

Certain well-defined and universal physical conditions and geometric relationships exist that control the size of the same class of nanostructures as well as the formation of different classes of nanostructures. One design principle underlying the formation of nanotubes lies in the control of their radii. The tube radius can be designed a priori because it equals, in principle, the bending radius of curvature of a given strained bilayer film. This principle has been applied by Deneke et al., who fabricated a series of InGaAs/GaAs nanotubes with radii ranging from 10 to 300 nm.[8] Our further analysis shows that there actually exists a maximum bending curvature for a given set of film-thickness combinations, which sets a theoretical limit on the smallest nanotube one can produce. It will be interesting for future experiments to confirm such a limit.

The design principles for fabricating different classes of nanostructures are more complex. Let us analyze the principles governing the formation of nanotubes/nanorings versus nanodrills/nanocoils in terms of the geometric and elastic properties of the bilayer film. Qualitatively, one can expect that the film is more likely to fold into a nanotube or nanoring if the film is wide, while it may fold into a nanodrill or nanocoil only if it is narrow. Thus, there must exist a design principle in terms of the film width, and more generally in terms of the film dimensions, which separates the formation of a nanotube from a nanocoil.

To illustrate this point, we examine the relative stability of a nanotube versus a nanocoil for given film dimensions of length L, width W, and thickness t, as shown in Figure 2. The characteristic bending curvature of a strained bilayer film depends on misfit strain (ε) and the thickness and elastic constants of the two constituting layers. If we assume, for simplicity, that the two layers have the same thickness ($t/2$) and elastic constants, the characteristic curvature, K, can be calculated as $K = -(3\varepsilon)/(2t)$.[18–21] Then, the film will fold into a tube or coil whose turns have a characteristic radius $R_0 = 1/K$ and a perimeter length $L_0 = 2\pi R_0$.

Whether the film will fold into a tube or coil is uniquely controlled by some intrinsic relations between the film geometric dimensions (e.g., W) and its characteristic bending scales (e.g., L_0). First, let's consider the film to be elastically isotropic, so that it may fold along any direction with equal bending energy. In this case, a coil can always be energetically favored to form over a tube when $W < L_0$. This is because the

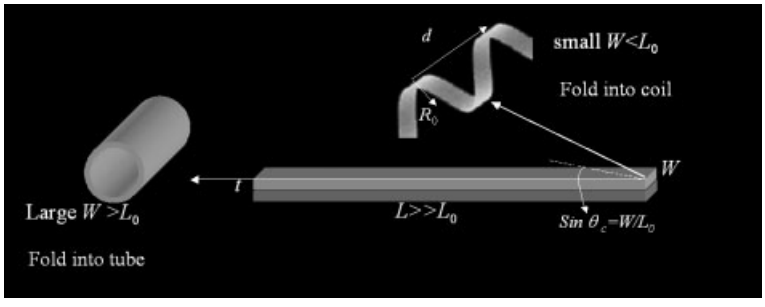

Figure 2. Schematic illustration of a strained bilayer film folding into a nanotube when W is large, but into a coil when W is small. The arrows indicate the folding direction.

ADVANCED MATERIALS

film can always fold into a coil by choosing a folding direction that has an angle, θ, with the film long edge larger than a critical angle θ_c defined as $\theta_c = \sin^{-1}(W/L_0)$, as shown in Figure 2, so that all the turns of the coil adopt the optimal radius R_0 with the minimum bending energy. In contrast, if the film folds into a tube with multiple turns by folding along a direction that makes an angle with its long edge that is smaller than θ_c, only its first turn can adopt R_0, while additional turns must adopt a radius larger than R_0 with the extra cost of bending energy. Therefore, there exist two critical geometric conditions for coil formation, i.e., $W < L_0$ and $\theta > \theta_c$. The spiral angle of the coil depends on the folding direction according to $\alpha = \tan^{-1}(d/R_0)$ (where $d \geq W$), as shown in Figure 2, and the minimum allowed spiral angle for any coil is $\theta = \tan^{-1}(W/R_0)$. If W and L are comparable, and both are larger than L_0, then the film may fold randomly along any direction, as we have observed in experiments.[22]

Next, we consider the film to be elastically anisotropic. In this case, the film is energetically preferred to *only* fold along the elastically most compliant direction. This adds another variable to the design principle for formation of nanotubes versus nanocoils, which now depends critically on the alignment between the most compliant direction and the film long edge. If the most compliant direction forms an angle with the film long edge which is larger than θ_c, then the film folds naturally along its most compliant direction into a coil as discussed above; otherwise, the film folds naturally into a tube.

Now, we demonstrate controlled experimental fabrication of nanorings versus nanocoils in order to validate the design principles based on elastic anisotropy, as also previously shown.[6,15] We use ultrathin Si/SiGe bilayer films as a model system, which are grown by molecular beam epitaxy (MBE) and chemical vapor deposition (CVD) onto a sacrificial SiGe on insulator (SGOI) substrate. Based on the elastic anisotropy of Si and Ge, we pattern the thin films into cantilevers of two different orientations: one along the (100) direction (Fig. 3, upper left), i.e., the most compliant direction of Si and Ge, and the other along the (110) direction (Fig. 3, upper right). The cantilevers are then released by etching, which bend upward and fold into nanorings or nanocoils.

As designed a priori, Figure 3 (left panel) shows that the (100)-orientated cantilevers fold naturally along the most compliant (100) direction into nanorings. All three cantilevers fold with the same characteristic radius, with the longest cantilever (20 μm) forming a complete ring and the two shorter cantilevers (15 μm) forming partial rings. In contrast, the two longest (110)-orientated cantilevers fold into nanocoils (Fig. 3, right panel), because the film tends to fold along the more-compliant (100) direction. The radius of nanocoils (~2.8 μm) is slightly smaller than that of nanorings (~3.2 μm), because the characteristic bending radius of the (110) cantilever is smaller than that of the (100) cantilever for the given thickness ratio, also consistent with theory.

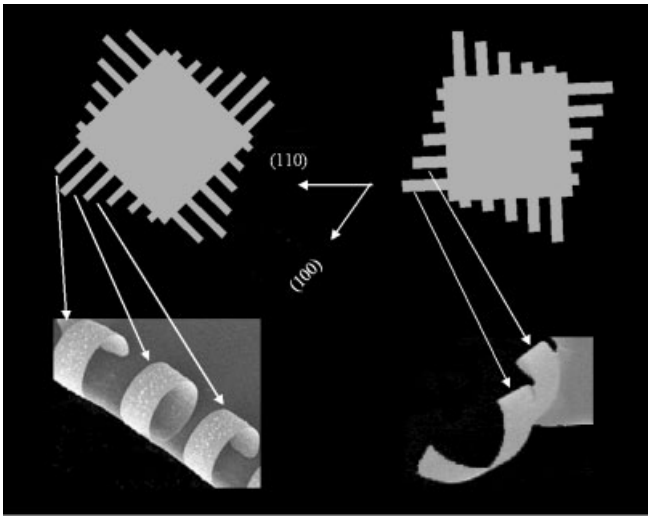

Figure 3. Experimental demonstration of strained Si/SiGe bilayer cantilevers folding into nanorings when they are patterned along (100) direction, but into nanocoils when they are patterned along (110) direction, as they prefer to fold along the more-compliant (100) direction. The nanorings have a thickness of 60 nm, a radius of ~3.2 μm, and a width of 3 μm; the nanocoils have a thickness of 76 nm, a radius of ~2.8 μm, and a width of 4 μm.

So far, we have considered the film to fold naturally with only the bending distortion. In addition, the film may also fold with shear distortion under external forces, in particular to form a coil. Then, the scenario for tube formation versus coil formation becomes much more complex. Let's consider a particular case when the film is most compliant in the direction along its long edge so that without shearing it will naturally fold into a tube, as discussed above. Apparently, only the first turn has the optimal radius of bending with the minimized bending energy, while others have radii that are too large. Thus, the nanotube forms with *an energy penalty of bending*.

Alternatively, one may pull the nanotube along its axial direction into a coil by an external force (e.g., using an AFM tip), so the film effectively folds into a nanocoil by bending plus shearing. In this case, all the turns can adopt the same optimal radius of bending, R_0, but each turn is sheared relative to its neighboring rotations by a minimum shear strain of $\pm W/L_0$. Consequently, the bending energy in the nanocoil is minimized in all the turns, but at an extra energy cost due to shearing. Thus, the nanocoil forms with *an energy penalty of shearing*.

We have calculated the total energy of a nanotube versus a nanocoil, as a function of the film length, width, and thickness. For the nanotube, the first turn has a radius of R_0, and the nth

turn has a radius of $R_0 + (n-1)t$. A film of total length, L, will fold into a nanotube of N turns, with

$$L = \sum_{n=1}^{N} 2\pi(R_0 + (n-1)t) \quad (1)$$

Assuming the two layers have the same thickness and elastic constants, the bending energy in the first turn can be analytically solved as

$$E_b = \frac{1}{32} M_b \varepsilon^2 (L_0 W t) \quad (2)$$

while the total energy needs to be numerically calculated by summing over bending energy in all N turns. For the nanocoil, its total energy consists of both bending and shearing energy. They are the same in all turns and can be calculated analytically as

$$E = \frac{1}{32} M_b \varepsilon^2 (LWt) + \frac{1}{2} M_s \gamma^2 (LWt) \quad (3)$$

where M_b and M_s are, respectively, the bending modulus (along the most compliant direction) and the shearing modulus, and $\gamma = d/L_0 \geq W/L_0$ is the shear strain associated with coiling (see Fig. 2).

Figure 4 shows the calculated "phase diagram" for a 60 nm thick Si/Ge bilayer film, defining the geometric regimes for nanotube versus nanocoil formation. For a given film length,

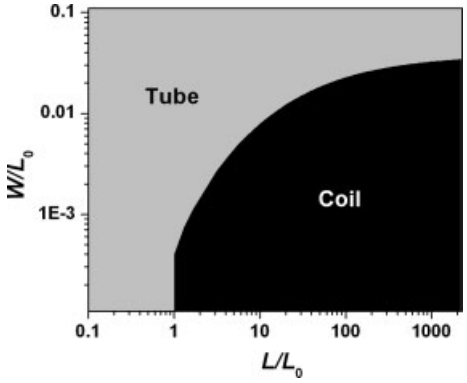

Figure 4. Log–log plot of the phase diagram of nanotubes and nanocoils as a function of reduced film length L/L_0 and reduced width W/L_0.

there exists a critical film width above which nanotubes form and below which nanocoils form. Conversely, for a given film width, there exists a critical film length. The minimum length for coil formation is L_0. There exists an upper limit of film width for nanocoil formation, above which only nanotubes form. The maximum width for coil formation is only about 3 % of L_0, indicating that the nanocoil is generally much harder to form by shearing when the most compliant direction is aligned with the long edge of the film.

The phase diagram defines the thermodynamic limit for nanotube versus nanocoil formation, in terms of film length and width. In reality, external force is needed to transform the naturally folded tube (kinetically limited) into a more stable coiling state. In addition to film dimensions, the phase diagram depends also on film elastic properties. For example, the phase boundary line in Figure 4 will shift upward with either decreasing shear modulus or increasing bending modulus. More generally, the coiling condition depends on the angle made between the most-compliant direction and the film long edge.

Besides the *intrinsic* geometric and physical conditions, the nanomechanical architecture of strained bilayer films also depends on *extrinsic* processing parameters. One important processing parameter is the etching rate, because the final bent structure depends on the rate of strain relaxation (i.e., the rate of stress waves) relative to the etching rate (i.e., the rate of the film being released from the sacrificial substrate). Both our computer simulations and experiments[22] show that the freed film must have a long enough relaxation time to roll into a tube, requiring the etching rate to be sufficiently slow. If the etching rate is too fast, the film may peel off the substrate into ripples instead of rolling into a tube. It is also possible to release the film from both ends to form a pair of the same nanostructures[23] or new types of nanostructures. We have been applying computer simulations as an effective tool to test the theoretical design principles and to explore novel nanometer-scale objects.

In summary, we have demonstrated by both theory and experiment some generic design principles for a novel nanofabrication approach, the nanomechanical architecture of strained bilayer films, in terms of geometric, physical, and processing parameters. Our theoretical analyses show that there exist fundamental geometric and physical conditions controlling the formation of nanotubes (nanorings) versus nanocoils (nanodrills). For an elastically isotropic film, the critical geometric condition for nanocoil formation is that the film width must be smaller than $L_0 = 2\pi R_0$, where R_0 is the characteristic bending radius of the given bilayer film. For an anisotropic film, nanocoil formation depends critically on the alignment of the most compliant direction of the film with respect to the film geometry (i.e., its long edge). We experimentally validate these design principles by fabricating nanorings, nanocoils, and nanodrills using advanced growth, patterning, and etching techniques. Furthermore, we construct the theoretical phase diagram for nanocoil formation with additional shear distortion under external forces.

We believe the nanomechanical architecture of strained bilayer thin films will become one of the most viable nanofabrication techniques in the future because of its unparalleled versatility in making a variety of different nanostructures from combinations of different classes of materials and its unprecedented level of control, allowing fabrication of nanostructures designed a priori. Our study not only contributes to the advancement of this emerging nanofabrication approach, but also has important implications for other existing approaches, especially for fabrication and synthesis of various nanotubes, nanobelts, and nanorings.

ADVANCED MATERIALS

Experimental

All the bilayer films were grown by deposition of Si onto a SiGe strained-layer on insulator (SGOI) using solid-source molecular-beam epitaxy (MBE), except for the one shown in Figure 3 (lower right) which was prepared by ultrahigh-vacuum chemical vapor deposition (UHV-CVD) growth of a Si/SiGe bilayer onto SOI. Both MBE and CVD SiGe films had a concentration of ~20 % Ge. The thicknesses of the CVD film were ~30 nm Si/~36 nm SiGe, determined by X-ray diffraction. For the MBE films, we were able to grow five different thickness (20, 40, 50, 70, and 100 nm) of Si layers in situ onto a single piece of SGOI substrate by rotating a shutter in an MBE chamber, allowing the film to fold with different characteristic bending radii. The growth rate was 0.55 Å s^{-1} at a substrate temperature of 585 °C, measured by an optical pyrometer. The MBE/CVD growth of the Si layer was monitored by reflection high-energy electron diffraction during the entire growth process.

The SGOI substrate was a free sample from SOITEC. The thickness and composition of SGOI were about 44 nm Si with 20 % Ge on 190 nm SiO_2. The sample was cleaned with 10 % hydrofluoric acid to remove the native oxide grown in air on the original SGOI surface, followed by 10 min of cleaning with piranha (H_2SO_4/H_2O_2), and a few seconds 10 % HF etching to remove the oxide layer produced during the piranha treatment. For UHV-CVD growth, we added an additional 15 min SC1 ($NH_4OH/H_2O_2/H_2O$ mixture) cleaning step at ~80 °C and deliberately dipped the sample into diluted HF acid to terminate the surface with hydrogen before loading it into the CVD chamber in order to prevent the growth of native oxide in air.

We performed photolithography and electron-beam lithography to pattern the thin films into cantilevers. Basically, an array of cantilevers with different dimensions and orientations was created on each side of a 50 μm × 50 μm square, as shown in Figure 3. The common width of the (100) cantilever was 3 μm and the lengths varied from the longest to the shortest as 20, 15, 10, 6, and 3 μm. The spacing in between was 5 μm. The width of the (110) cantilever was 6 μm and the length varied as 36, 26, 16, 6, and 4 μm. The spacing in between was 2 μm.

After lithography, the desired patterns were transferred onto the $Si/Si_{0.8}Ge_{0.2}$ bilayer film by using O_2 and SF_6 reactive-ion etching. The underlying sacrificial oxide layer was selectively etched off by the vapor of HF acid to release the cantilever, which bended upward and folded into nanorings or nanocoils. The HF vapor releasing process was carried out at a temperature of 40 °C with a time duration of 30–60 min. The most important advantage of this technique is that it is a single process without subsequent rinsing steps, thus preventing the released structure from sticking onto the substrate. Also, for this purpose, it was necessary to create a strain configuration, with a Si film grown on top of SiGe by using the unique SGOI wafer. In the normal configuration, with a SiGe film grown on top of Si by using the conventional SOI wafer, the released bilayer film would bend downward so that it was blocked from folding completely.

Received: June 30, 2005
Final version: August 24, 2005
Published online: October 19, 2005

[1] S. Fan, M. G. Chapline, N. R. Franklin, T. W. Tombler, A. M. Cassell, H. Dai, *Science* **1999**, *283*, 512.
[2] X. Y. Kong, Y. Ding, R. Yang, Z. L. Wang, *Science* **2004**, *303*, 1348.
[3] L. Bai, J. Tersoff, F. Liu, *Phys. Rev. Lett.* **2004**, *92*, 225 503.
[4] B. Yang, F. Liu, M. G. Lagally, *Phys. Rev. Lett.* **2004**, *92*, 025 502.
[5] J. Liu, S. S. Fan, H. J. Dai, *MRS Bull.* **2004**, *29*, 244.
[6] V. Y. Prinz, V. A. Seleznev, A. K. Gutakovsky, A. V. Chehovsky, V. V. Preobrazhenskii, M. A. Putyato, T. A. Gavrilova, *Physica E* **2000**, *6*, 828.
[7] O. G. Schmidt, K. Eberl, *Nature* **2001**, *410*, 168.
[8] C. Deneke, C. Muller, N. Y. Jin-Phillipp, O. G. Schmidt, *Semicond. Sci. Technol.* **2002**, *17*, 1278.
[9] S. M. Jurga, C. H. Hidrovo, J. Niemczura, H. I. Smith, G. Barbastathis, *IEEE. Conf. on Nanotechnology*, **2003**, 2, 220.
[10] O. Schumacher, S. Mendach, H. Welsch, A. Schramm, C. Heyn, W. Hansen, *Appl. Phys. Lett.* **2005**, *86*, 143 109.
[11] O. G. Schmidt, N. Schmarje, C. Deneke, C. Muller, N. Y. Jin-Phillipp, *Adv. Matter.* **2001**, *13*, 756.
[12] O. G. Schmidt, C. Deneke, Y. M. Manz, C. Muller, *Physica E* **2002**, *13*, 969.
[13] S. V. Golod, V. Y. Prinz, P. Wagli, L. Zhang, O. Kirfel, E. Glaus, C. David, D. Grützmacher, *Appl. Phys. Lett.* **2004**, *84*, 3391.
[14] P. O. Vaccaro, K. Kubota, T. Aida, *Appl. Phys. Lett.* **2001**, *78*, 2852.
[15] L. Zhang, E. Deckhardt, A. Weber, C. Schönenberger, D. Grützmacher, *Nanotechnology* **2005**, *16*, 655.
[16] T. Tokuda, Y. Sakano, D. Mori, J. Ohta, M. Nunoshita, P. O. Vaccaro, A. Vorob'ev, K. Kubota, N. Saito, *Electron. Lett.* **2004**, *40*, 21.
[17] Here, the drill and coil are referred to as open structures with each rotation having the same radius without overlapping each other; the difference is that the drill (or coil) has a film width larger (or smaller) than the spacing between the rotations. In contrast, the tube has a closed structure with overlapping rotations of different radii that may or may not be shifted with respect to each other.
[18] S. Timoshenko, *J. Opt. Soc. Am.* **1925**, *11*, 233.
[19] F. Liu, P. Rugheimer, E. Mateeva, D. E. Savage, M. G. Lagally, *Nature* **2002**, *416*, 498.
[20] F. Liu, M. Huang, P. Rugheimer, D. E. Savage, M. G. Lagally, *Phys. Rev. Lett.* **2002**, *89*, 136 101.
[21] M. H. Huang, P. Rugheimer, M. G. Lagally, F. Liu, *Phys. Rev. B: Condens. Matter Mater. Phys.* **2005**, *72*, 085 450.
[22] H. Qin, N. Shaji, N. E. Merrill, H. S. Kim, R. C. Toonen, R. H. Blick, M. M. Roberts, D. E. Savage, M. G. Lagally, G. K. Celler, unpublished.
[23] G. Schmidt, C. Deneke, S. Kiravittaya, R. Songmuang, H. Heidemeyer, Y. Nakamura, R. Zapf-Gottwick, C. Muller, N. Y. Jin-Phillipp, *IEEE J. Sel. Top. Quantum Electron.* **2002**, *8*, 1025.

Carbon Nanofibers Allow Foaming of Semicrystalline Poly(ether ether ketone)

By *Philipp Werner*, *Raquel Verdejo*, *Frank Wöllecke*, *Volker Altstädt*, *Jan K. W. Sandler*,* and *Milo S. P. Shaffer**

Carbon nanotubes (CNTs) and carbon nanofibers (CNFs) have intrinsic potential to reinforce fine structures where other reinforcements cannot be accommodated. In this study, a CNF-filled semicrystalline polymer foam has been produced

[*] Dr. J. K. W. Sandler, Prof. V. Altstädt
Polymer Engineering, University of Bayreuth
Universitätsstrasse 30, D-95447 Bayreuth (Germany)
E-mail: jan.sandler@uni-bayreuth.de
Dr. M. S. P. Shaffer, Dr. R. Verdejo
Department of Chemistry, Imperial College
London, SW7 2AZ (UK)
E-mail: m.shaffer@imperial.ac.uk
Dr. P. Werner, Dr. F. Wöllecke
Basell Polyolefine GmbH
Industriepark Höchst
C657, D-65926 Frankfurt (Germany)

  DOI: 10.1002/adma.200500709